Anbar Journal Of Engineering Science©

journal homepage: http://www.uoanbar.edu.iq/Evaluate/

Unviersty of Anbar

Numerical Study on the Convective Heat Transfer of Nanofluid Flow in Channel with Trapezoidal Baffles

Munjid K. Mohammed [a]*, M. A. Ahmed [a]

[a] Department of Mechanical Engineering, College of Engineering, University of Anbar Ramadi, Anbar, Iraq

P A P E R I N F O

Paper history:
Received 13 march 2018
Received in revised form 13 April 2018
Accepted 23 April 2018

Keywords:
Trapezoidal baffles
Nanofluid
Thermal-hydraulic performance
Laminar Flow
Finite volume method

A B S T R A C T

This article presents a numerical study on forced convection of nanofluid flow in a two-dimensional channel with trapezoidal baffles. One baffle mounted on the top wall of channel and another mounted on the bottom wall of channel. The governing continuity, momentum and energy equations in body-fitted coordinates are iteratively solved using finite volume method and SIMPLE technique. In the current study, SiO_2-water nanofluid with nanoparticles volume fraction range of 0- 0.04 and nanoparticles diameters of 30 nm is considered for Reynolds number ranging from 100 to 1000. The effect of baffles height and location, nanoparticles volume fraction and Reynolds number on the flow and thermal fields are investigated. It is found that the average Nusselt number as well as thermal hydraulic performance increases with increasing nanopartiles volume fraction and baffle height but accompanied by increases the pressure drop. The results also show that the best thermal- hydraulic performance is obtained at baffle height of 0.3 mm, locations of baffles at upper and lower walls of 10 and 15 mm, respectively, and nanoparticles volume fraction of 0.04 over the ranges of Reynolds number.

1. Introduction

Heat transfer enhancement is an extremely significant issue in many engineering application, especially those using heat exchangers. Fluid flow past baffles, small turbulator or cavities in a channel were take scopes wide of studies topic of intense research during 100 along years improve in thermal performance in such device. In recent years, even more enhancement in the performance of heat exchangers are sought in order to meet all the industries requirements and demands for a higher thermal performance in such devices. However, changing in geometrical parameters to enhance the performance of heat exchangers has reached the optimum limit. Research on the method for further enhancement in heat transfer has become fundamental. On coolant side, the low thermal conductivities of traditional heat transfer fluids (such as water, oil and ethylene glycol) are considered as a fundamental obstacle to improve heat exchangers performance. Forced convectional flows in channel with different shapes of turbulators are experimentally and numerically studied by many researchers. Habib et al. [1] studied experimentally on turbulent flow and heat transfer characteristics in a rectangular duct with staggered baffles and found that the pressure losses and heat transfer coefficient increase with the increase of the baffle height. Zhu et al. [2] numerically investigated on the turbulent flows and heat transfer in a rib-roughened channel with longitudinal vortex generators and it is observed that the combined effect of the rib- roughness and the vortex generators can improve the rate of heat transfer. Korichi and Oufer [3] numerically studied of the heat transfer enhancement in channel with obstacles mounted on the walls of channel and results showed that the rate of heat removed from the obstacles increases with Reynolds number. Somchai and Pongjet [4] studied numerically on the laminar heat transfer in a channel with diamond-shaped baffles and it is observed that reduction of the baffles angles of diamond leads to increase Nusslet number and the friction factor. Oztop et al. [5] performed a numerical investigation on laminar forced convection heat transfer and fluid flow characteristics in channel with heated blocks mounted on its bottom wall and showed that the result the rate of heat transfer enhanced for all Reynolds number. Promvonge et al. [6] conducted a numerical investigation of the fluid flow and heat transfer in a square channel with 45° inline baffles on two opposite walls and the result showed the values of the Nusslet number and friction factor increase with increase in height baffles. Heidary and Kermani [7] numerically studied the effect of blocks at the lower wall of channel with utilizing nanofluid flow on the local and average Nusslet number and results showed that the highest heat transfer enhancement about 60% was obtained with using blocks and nanofluid in channel. Lei et al. [8] conducted a numerical and experimental investigation on the heat transfer enhancement in microchannel heat sinks with periodic expansion-constriction cross-sections and found the heat transfer enhanced with using periodic expansion-constriction cross-sections. Islami et al. [9] studied numerically the laminar flow and heat transfer of Al_2O_3-water nanofluid in a microchannel with and without micromixers. In this study the baffles mounted on the upper and lower walls of channel and it was found that using nanoparticles and baffles can improve the heat transfer rate but the friction factor increases as well. Heshmati et al [10] investigated numerically on mixed convection heat transfer of nanofluid over the backward facing step with slotted baffles and the results showed that the rate of heat transfer enhanced with using inclined lotted baffles. Hamdi and Yusoff [11] studied numerically on the convective heat transfer of Al_2O_3-water nanofluid flow in a triangular channel using vortex generators and the result showed that the heat transfer rate is dependent on the concentration of nanoparticle and the attack angle of vortex generators. Khoshvaght-Aliabadi et al. [12] studied experimentally and numerically of the for the laminar force convection of copper-water nanofluid flow in plate-fin heat exchanger with vortex-generator. The result showed that the best the thermal performance was obtained with the use wings at the angle of attach of 60°. Ahmed et al. [13-19] numerically conducted on the nanofluid flow in a corrugated channel and observed that the heat transfer enhanced with using corrugated channel and with suspension nanoparticle. Mohammed et al. [20] conducted a numerical investigation on the mixed convection of nanofluid flow over backward facing step with rectangular baffles. They observed the baffle height, baffle distance and baffle location have an important effect on heat transfer enhancement, while the baffle width has no important effect. Abdollahi and Shams [21] numerically studied on the effect of the vortex generators on the heat transfer enhancement in rectangular channel using nanofluid and found that the performance of channel improved with the volume fraction of nanoparticles and with using vortex generator. Wang and Zhao [22] studied on the performance of rectangular channel with using circular cylinder as vortex generators and result showed that the thermal performance of channel enhanced with using vortex generator. Esfe et al. [23] carried out a numerical study of the laminar mixed convection nanofluid flow in a horizontal channel with two hot obstacles mounted at the lower wall. They observed the highest augmentation in heat transfer was less than 10% as a nanoparticles volume friction increase from 0 to 5%. Khoshvaght-Aliabadi et al. [24] experimentally conducted on the effect of the corrugated/ vortex generators of plate-fin on the thermal- hydraulic characteristic of plate fin heat exchangers and they observed that the highest improvement in the rate of heat transfer was about 83.7% for corrugated/vortex generators plate fine heat exchanger as a compared to the smooth channel. Datta et al. [25] numerically investigated of the heat transfer augmentation in microchannel using vortex generator and it was found that the best thermal performance has been obtained at Reynolds number of 600 with angle of longitudinal vortex generator of 30^{o}.

In current study, the laminar forced convection flow of SiO_2-water nanofluid in a two-dimensional channel with trapezoidal baffles is numerically stdied. The effect of geometrical parameter of baffles such as height of baffles as well as and the location of baffles, Reynolds number and volume fraction of nanoparticles on the flow and thermal fields are investigated.

2. Mathematical formulation

2.1 Physical model and assuptions

In this study the physical model is consisting of two

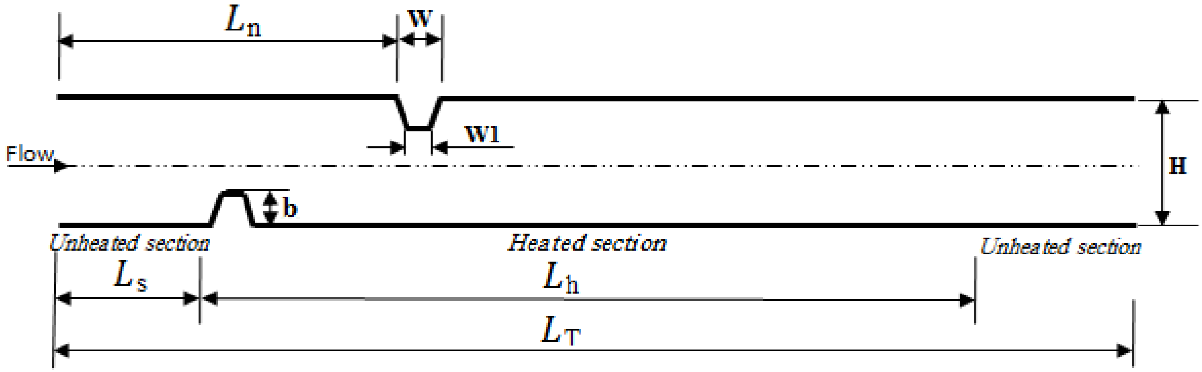

Figure 1. Physical domain for the current study.

parallel plates with spacing (H) is 1 mm and the total length (L_T) is 30 mm as shown in the Fig. 1. The channel is consisting of three sections; unheated section, heated section and unheated section. The length of the heated section (L_h) is 20 mm, while the length of each unheated sections is 5 mm. The two identical baffels with trapezoidal shapes are mounted at the upper and lower walls of heated section with different distances from the entrance of channel. The lower baffle is located at different distances from the entrance of channel (L_s= 5, 10 and 15mm), while the upper baffles is located at the distance (L_n) 10 mm from the entrance of channel. The baffles widths are W=1 mm and w_1=0.5 mm, while the baffles height (b) of 0, 0.1, 0.2 and 0.3 mm. It can be assumed that the flow is, steady, laminar, incompressible, and two-dimensional. In addition, the cold mixture of base fluid (water) and the spherical nanoparticles of SiO_2 can be assumed as a homogenous mixture.

2.2 Governing equations

The governing equations in term of body-fitted coordinate system form are given as [26]:

- Continuity:

$$\frac{\partial(U^c)}{\partial\zeta}+\frac{\partial(V^c)}{\partial\eta}=0 \qquad (1)$$

X-Momentum

$$\frac{\partial(UU^c)}{\partial\zeta}+\frac{\partial(UV^c)}{\partial\eta}=\frac{1}{Re}\left[\frac{\partial}{\partial\zeta}\left(B_{11}\frac{\partial U}{\partial\zeta}\right)+\frac{\partial}{\partial\eta}\left(B_{22}\frac{\partial U}{\partial\eta}\right)+\frac{\partial}{\partial\zeta}\left(B_{12}\frac{\partial U}{\partial\eta}\right)+\frac{\partial}{\partial\eta}\left(B_{12}\frac{\partial U}{\partial\zeta}\right)\right]-\left[B_{11}\frac{\partial P}{\partial\zeta}+B_{12}\frac{\partial P}{\partial\eta}\right] \qquad (2)$$

Y-Momentum:

$$\frac{\partial(VU^c)}{\partial\zeta}+\frac{\partial(VV^c)}{\partial\eta}=\frac{1}{Re}\left[\frac{\partial}{\partial\zeta}\left(B_{11}\frac{\partial V}{\partial\zeta}\right)+\frac{\partial}{\partial\eta}\left(B_{22}\frac{\partial V}{\partial\eta}\right)+\frac{\partial}{\partial\zeta}\left(B_{12}\frac{\partial V}{\partial\eta}\right)+\frac{\partial}{\partial\eta}\left(B_{12}\frac{\partial V}{\partial\zeta}\right)\right]-\left[B_{11}\frac{\partial P}{\partial\zeta}+B_{12}\frac{\partial P}{\partial\eta}\right] \qquad (3)$$

Energy:

$$\frac{\partial(\theta U^c)}{\partial\zeta}+\frac{\partial(\theta V^c)}{\partial\eta}=\frac{1}{Re\,Pr}\left[\frac{\partial}{\partial\zeta}\left(B_{11}\frac{\partial\theta}{\partial\zeta}\right)+\frac{\partial}{\partial\eta}\left(B_{22}\frac{\partial\theta}{\partial\eta}\right)+\frac{\partial}{\partial\zeta}\left(B_{12}\frac{\partial\theta}{\partial\eta}\right)+\frac{\partial}{\partial\eta}\left(B_{21}\frac{\partial\theta}{\partial\zeta}\right)\right] \qquad (4)$$

Where:

$$U^c=UY_\eta-VX_\eta\,,\quad V^c=VX_\zeta-UY_\zeta\,,$$

$$J=X_\zeta Y_\eta-X_\eta Y_\zeta \qquad (5)$$

$$B_{11}=\frac{({X_\eta}^2+{Y_\eta}^2)}{J}\,,\quad B_{22}=\frac{({X_\zeta}^2+{Y_\zeta}^2)}{J}\,,$$

$$B_{12}=B_{21}=-\frac{(X_\zeta X_\eta+Y_\zeta Y_\eta)}{J} \qquad (6)$$

The non-dimensional quantities that are used in the above equations can be expressed as:

$$X = \frac{x}{D_h}, \quad Y = \frac{y}{D_h}, \quad U = \frac{u}{u_{in}},$$

$$\theta = \frac{T - T_{in}}{T_w - T_{in}}, \qquad P = \frac{p}{\rho_{nf} u_{in}^2} \tag{7}$$

In order to solve the above governing equations used in the current study, the boundary conditions are defined as:

i. At the entrance of channel:

$$U = \frac{3}{2}[1 - \frac{y}{H/2}]^2 \text{ , where } -H/2 \le y \le H/2$$

$$V = 0, \ \theta = 0 \tag{8a}$$

ii. At the outlet of channel:

$$\frac{\partial U}{\partial X} = 0, \ \frac{\partial V}{\partial X} = 0, \ \frac{\partial \theta}{\partial X} = 0 \tag{8b}$$

iii. At the walls of channels:

$$U = 0, V = 0, \ \theta = 1 \tag{8c}$$

The thermophysical properties of SiO2-water nanofluid considered in the current study are the ones used by Navaei et al. [27].

3. Numerical algorithm

The governing equations in terms of body fitted co-ordinate system have been solved using finite volume approach based on SIMPLE algorithm [28]. The collocated grid arrangement is used to store all physical variables, such as velocities, temperature and pressure, in the same nodes of computational domain [29]. Further, the Poisson equations are solved to develop the computational grid of present study, see Fig. 2. The under-relaxation of all physical variables is applied to converge the numerical solution. Thus, the convergence criterion for all variables is set to 10^{-5}. After solving the governing equations, some useful parameters can be determined. For example, the local Nusselt number at the walls of channel is determined as [30]:

$$Nu_x = \frac{h_x D_h}{k_{nf}} = -\frac{k_{nf}}{k_f}\frac{\partial \theta}{\partial y} \tag{9}$$

The average Nusselt number is defined as [16]:

$$Nu_L = \frac{1}{L}\int_{L_s}^{L_s+L_h} Nu_x \, dx \tag{10}$$

The friction factor is given as [31]:

$$f = \Delta p \frac{D_h}{L} \frac{2}{\rho_{nf} U_{in}^2} \tag{11}$$

The performance evaluation criterion is defined as [17]:

$$PEC = \frac{(Nu_{av} / Nu_{av,s})}{(f/f_s)^{1/3}} \tag{12}$$

4. Grid testing and code validation

In order to test the grid independent, the average Nusselt number are estimated for different grid sizes of (281×51, 381×51, 381×61, 481×61 and 481×71) as shown in Fig. 3. It is found the optimum grid sizes is 481×61, therefore it will be employed them throughout all computations of the current study. In order to check the accuracy of numerical algorithm that is used for simulating forced convection flow in channel with trapezoidal baffles, the average Nusselt number and friction factor for water flow in a wavy channel have been estimated and compared with previous with previous numerical and experimental results of Sui and et al. [32] as shown in Fig. 4. (a and b). It is observed the agreement between current and previous results is acceptable.

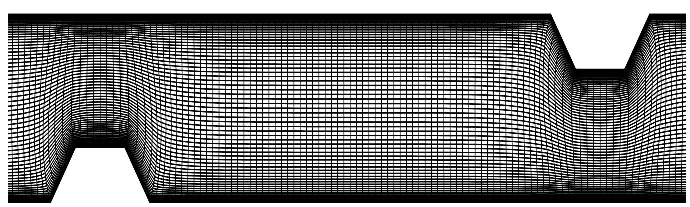

Figure 2. Computational Grid for the current study.

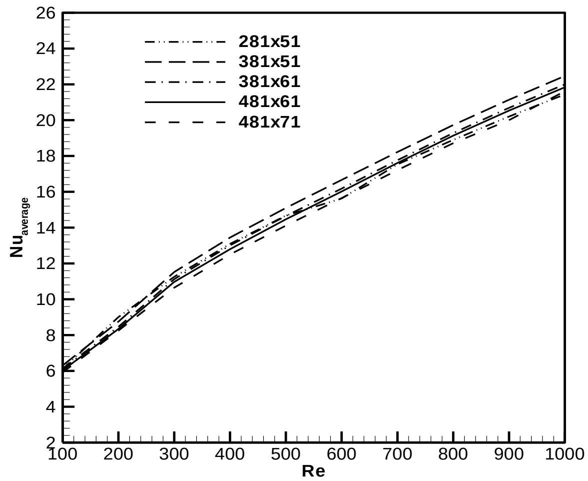

Figure 3. Average Nusselt number versus Reynols number for different grid sizes at L_n=10 mm, L_s=10 mm, b=0.3 mm, w=1 mm, w_1=0.5 mm and $\varphi = 4\%$.

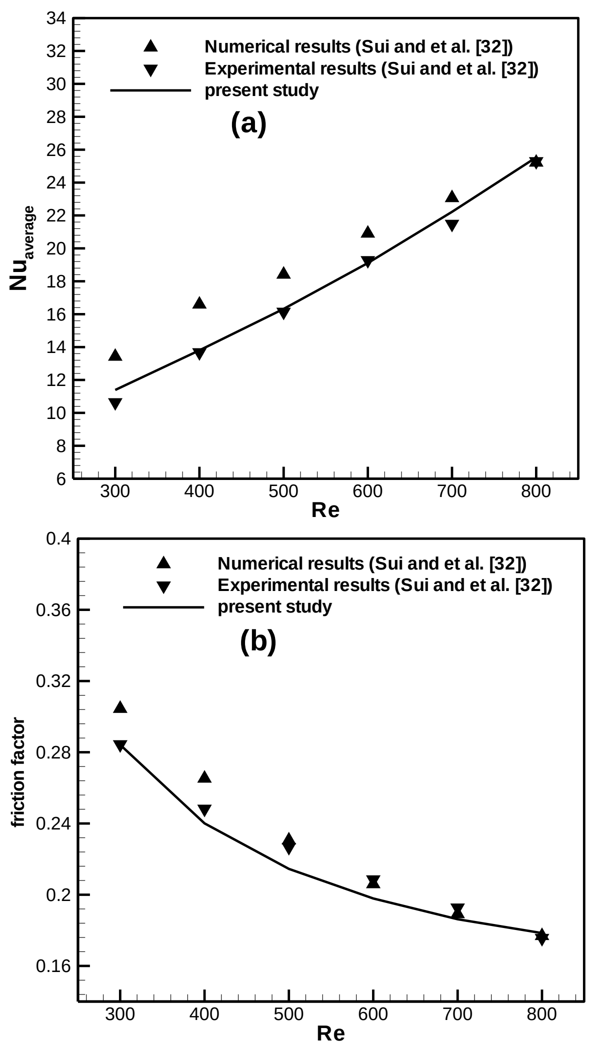

Figure 4. Comparison the present study with previous experimental and numerical study of Sui and et al. [32] (a) average Nusselt number and (b) friction factor.

5. Result and discussion

The effect of baffles height and the location, Reynolds number and nanoparticles volume fraction on the flow and thermal characteristics have been presented and discussed in current study. The velocity vector and isotherms contours at b=0.3 mm, L_n=10 mm, L_s=5 mm and $\varphi = 4\%$ as shown in Fig.5. It can be seen from the velocity vector that when the nanofluid flowing in channel, the re-circulation regions grows behind the upper and lower baffles. It is clearly observed that the direction of flow in these regions is in the opposite direction to the main flow. Furthermore, it is found that the size of re-circulation regions increases with increasing Reynolds number. Looking at isotherms contours, it can be noted that the thickness of thermal boundary layer decreases with increasing Reynolds number. It is also observed that the presence of the re-circulation zones can improve the mixing of the hot fluid at the walls and the cold fluid at the core. The effect of nanoparticles volume fraction on the average Nusselt number for different Reynolds number at L_n=10 mm, L_s=5 mm and b=0.3 mm is depicted in Fig.6a. As expected, it is observed that the average Nusselt number increases with Reynolds number. Also, the average Nusselt number increases with nanoparticles volume fraction due to enhance thermal conductivity of working fluid. Fig. 6.b displays the effect of nanoparticles volume friction on the non-dimensional pressure drop at L_n=10 mm and L_s=5 mm and b=0.3 mm. In general, the non-dimensional pressure drop is gradually decrease with Reynolds number. At a given Reynolds number, the pressure drop is slightly increased as nanoparticles volume fraction increase due to increase the viscosity of working fluid. The variation of thermal-hydraulic performance factor versus Reynolds numbers with different nanoparticles volume fraction at L_n=10 mm and L_s=5 mm and b=0.3 mm is shown in Fig. 6.c. It is found that the performance factor increases with nanopaprticles volume fraction because the enhancement in heat transfer is higher than increase in friction factor.

Fig. 7.a. displays the effect of baffle height on the average Nusselt number at L_n=10 mm, L_s=5 mm and$\varphi = 4\%$. As expected, it is also found that the minimum value of the average Nusselt number over Reynolds number when b=0, without baffle, because the poor fluid mixing in straight channel and hence higher thickness of the thermal boundary layer. The average Nusselt number increases with increasing the baffle height because of the size of re-circulation regions increases with baffle height and consequently enhance fluid mixing in channel. Fig. 7.b demonstrates the effect of baffle height on the non-dimensional pressure drop for different Reynolds

number at L_n=10 mm, L_s=5 mm and $\varphi = 4\%$. It is observed the pressure drop increases as the baffle height increase due to presence the re-circulation regions that growth behind the upper and lower baffle. The effect of baffle height on thermal-hydraulic performance for different Reynolds number at L_n=10 mm, L_s=5 mm and $\varphi = 4\%$ as depicts in Fig. 7.c. It can be seen that the thermal-hydraulic performance factor is greater than unity for any value of Reynolds as well as baffle height. This means that the augmentation heat transfer is greater than the pressure drop penalty. It can also be seen that the performance factor increases with the baffle height due to improve the fluid mixing in channel.

The effect of location of lower baffle on the average Nusselt number for different Reynolds number at b=0.3mm, L_n=10 mm and $\varphi = 4\%$ is depicts in Fig. 8.a. It can be observed that the location of baffles has a clear effect on the average Nusselt number. When the upper and lower baffles located at the same distance from the inlet of the channel (i.e. at L_s=10 mm and L_n=10 mm), the average Nusselt number has the highest value due to improve the fluid mixing as well as increase the velocity and temperature gradients. This is because the crosses sectional area of channel, at this location, is smaller than that for any location of lower baffle and hence increases the velocity and temperature gradients. Fig. 8.b displays the effect of location of the lower baffle on the non-dimensional pressure drops with Reynolds numbers for different at b=0.3 mm, L_n=10 mm and $\varphi = 4\%$. It is found that the pressure drop have the highest value at L_s=10 mm due to increase the velocity gradient at this location as pointed out earlier. Fig. 8.c shows the variation of thermal-hydraulic performance factor versus Reynolds number for different location of the lower baffle, respectively. In general, it is found that the performance factor is greater than unity for all values of the baffle distance considered in this study. This means that the enhancement in the heat transfer is higher than the increasing in friction losses. In addition, it is observed that the channel provides the best performance over Reynolds number range at L_s=15 mm and L_n=10 mm due to improve the mixing of fluid and hence enhance the heat transfer rate.

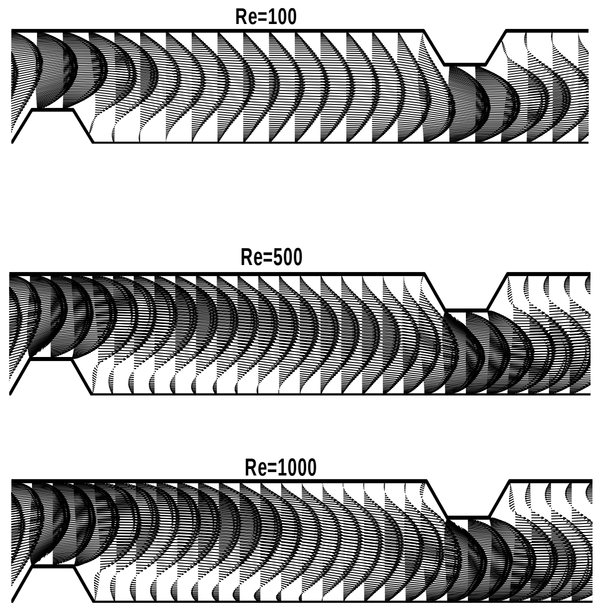

Figure 5. a. Velocity vector for different Reynolds numbers at L_n=10 mm, L_s=5 mm, b=0.3 mm and $\varphi = 4\%$.

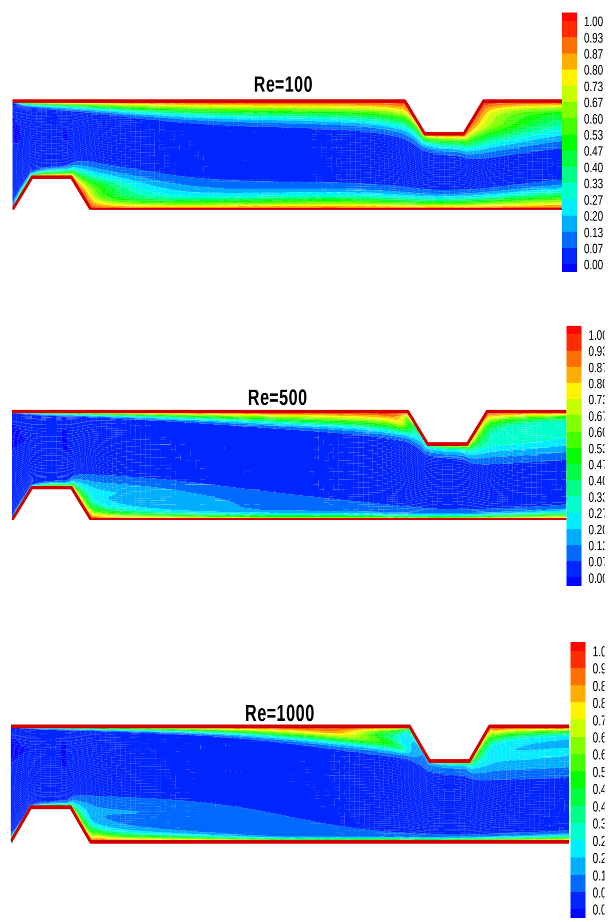

Figure 5. b. Isotherm contours for different Reynolds numbers at L_n=10 mm, L_s=5 mm, b=0.3 mm and $\varphi = 4\%$.

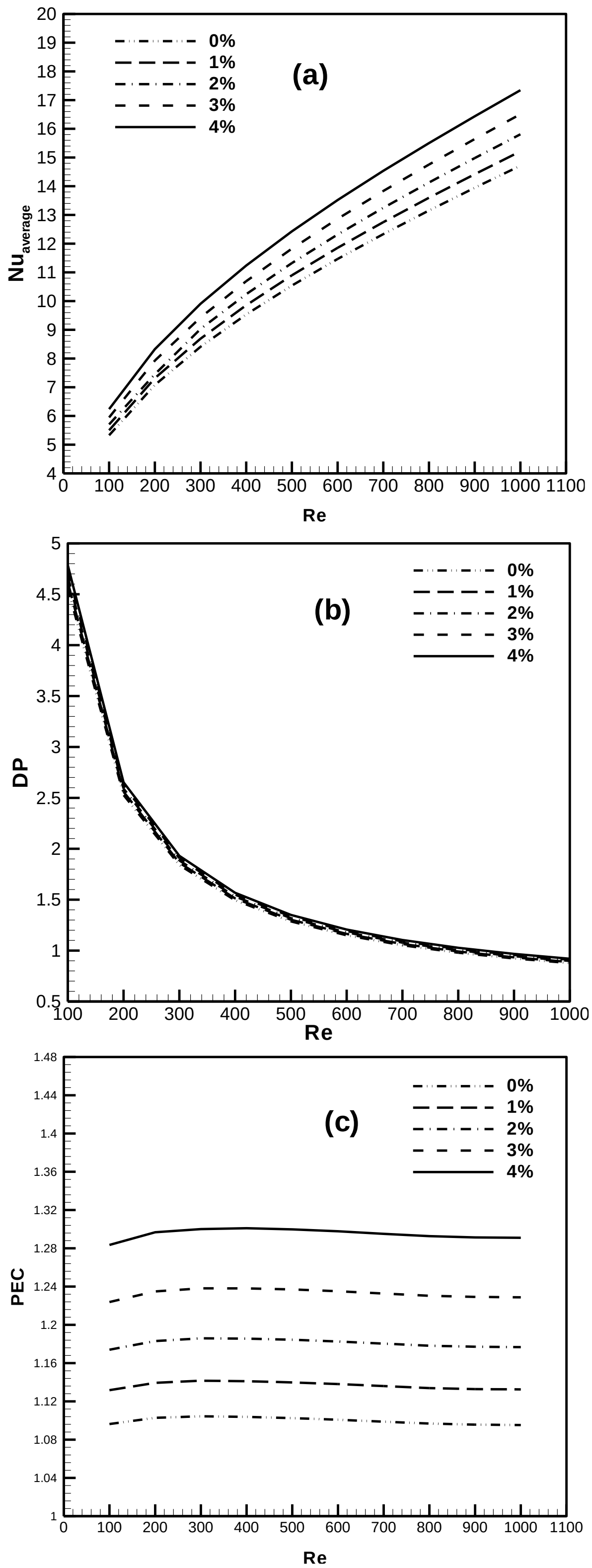

Figure 6. Effect of nanoparticles volume fraction on (a) average Nusselt number; (b) non-dimensional pressure drop; (c) Thermal- hydraulic performance factor at L_n=10 mm, L_s=5 mm, b=0.3 mm.

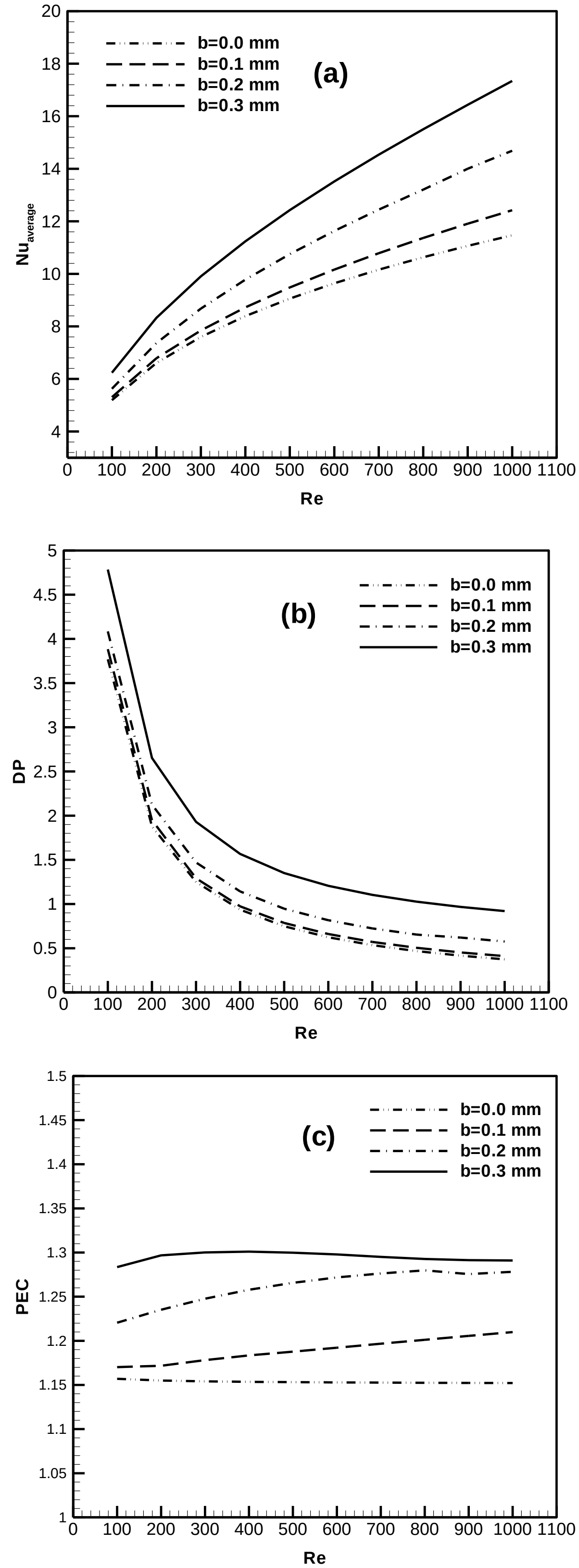

Figure 7. Effect of baffle height on (a) average Nusselt number; (b) non-dimensional pressure drop; (c) Thermal- hydraulic performance factor at L_n=10 mm, L_s=5 mm, φ=4%.

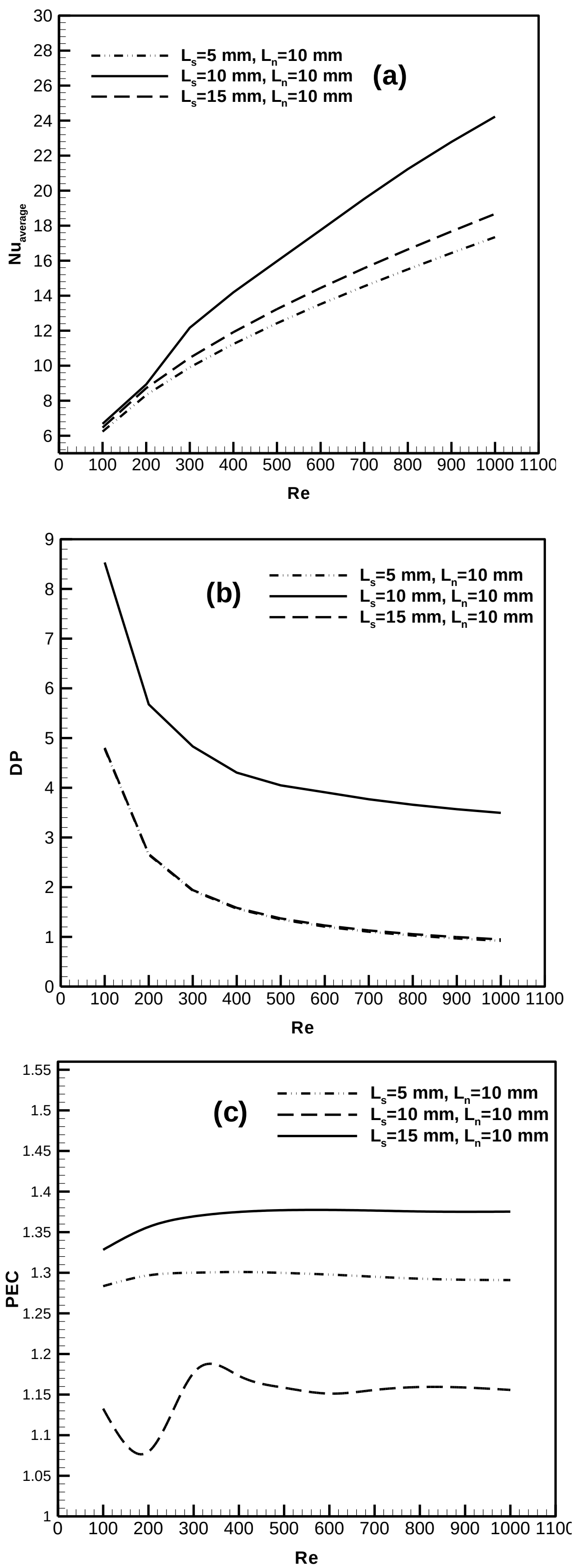

Figure 8. Effect of baffle location at the lower wall on (a) average Nusselt number; (b) non-dimensional pressure drop; (c) Thermal- hydraulic performance factor at L_n=10 mm, b=0.3 mm and φ=4%.

6. Conclusion

In this study, the flow and thermal characteristics of laminar nanofluid flow in a two-dimensional channel with trapezoidal baffles have been numerically studied over Reynolds number range of 100-1000. It is found that the average Nusselt number as well as thermal hydraulic performance increases with increasing nanopartiles volume fraction and baffle height but accompanied by increases the pressure drop. It also observed that the using trapezoidal baffles with height of 0.3 mm, locations at upper and lower walls of 10 mm and 15 mm, respectively, and nanoparticles volume fraction of 4% provide the best thermal-hydraulic performance. Therefore, it can be conclued that using nanofluid instead of conventional fluids in a channel with trapezoidal baffles can potentially lead to further improvement in the performance of heat exchangers with more compact design.

Nomenclature

b	baffle height, mm
C_p	Specific heat, J/kg.K°
D_h	hydraulic diameter, mm (D_h= 2H)
Dp	dimensionless pressure drop, (Dp=$\Delta p/\rho_{nf}\, u_{in}^2$)
f	friction factor
H	height of channel, mm
h	heat transfer coefficient, W/m^2.K°
K	thermal conductivity, W/m. K°
L_T	Total length of channel, mm
L_h	length of the duct heating, mm
L_n	distance to the baffle at upper wall
L_s	distance to the baffle at lower wall
Nu	Nusselt number, (Nu=h.D_h/K_f)
p	Pressure, (N/ m^2)
P	dimensionless pressure, (P= $P/\rho_{nf}\, U_{in}^2$)

Pr	Prandtl number, ($Pr = \mu_{nf} C_{p}/k_{nf}$)
PEC	thermal-hydraulic performance factor
Re	Reynolds number, ($Re = \rho_{nf}.U_{in}.D_h/\mu_{nf}$)
T_w	temperature at the wall of channel, K°
T	temperature of the fluid, K°
u, v	velocities components, m/s
U, V	dimensionless velocity component
W	width of the base baffle, mm
w_1	width of the top baffle, mm
x, y	2D Cartesian coordinates, mm
X,Y	dimensionless Cartesian coordinate
Greeks symbols	
ζ, η	Body fitted coordinates
B_{11}, B_{12}	Transforming coefficients
B_{22}, B_{21}	Transforming coefficients
β	friction of the liquid volume traveling with a particle
φ	volume friction of nanoparticles, %
α	Thermal diffusivity, ($\alpha = k/\rho.C_P$), m²/s
μ	dynamic viscosity, (N.s/ m²)
θ	dimensionless temperature
ρ	density, (Kg/m³)
Δp	Pressure drop, (N/ m²)
Subscripts	
ave.	average value
f	base fluid
in	inlet channel
nf	Nanofluid
p	Particles

References

[1] M.A. Habib, A.M. Mobarak, M.A. Sallak, E.A. Abdel Hadi, R.I. Affify, "Experimental investigation of heat transfer and flow over baffles of different heights," ASME J. Heat Transfer 116 (1994) 363–368.

[2] J. X. Zhu, M. Fiebig and N. K. Mitra, Numerical investigation of turbulent flows and heat transfer in a rib-roughened channel with longitudinal vortex generators. Int. J. Heat and Mass Transfer 38 (1995) 495-501.

[3] A. Korichi, L. Oufer, Numercal heat transfer in a rectangular channel with mounted obstacles on upper and lower walls, Int. J. Thermal sciences 44(2005) 644-655.

[4] S. Sripattanapipat, P. Promvonge, Numerical analysis of laminar heat transfer in a channel with diamond-shaped baffle, Int. J Heat Mass Transfer 36 (2009) 32-38.

[5] H.F. Oztop, Y. Varol, D.E. Alnak, Control of heat transfer and fluid flow using a triangular bar in heated blocks located in a channel, Int. Commun. Heat Mass Transfer 36 (2009) 878-885.

[6] P. Promvonge, S. Sripattanapipat, S. Kwankaomeng, Laminar periodic flow and heat transfer in square channel with 45° inline baffles on two opposite walls, Int. J. Thermal Science 49(2010) 963–975.

[7] H. Heidary, M. J. Kermani, Heat transfer enhancement in a channel with block (s) effect and utilizing Nano-fluid, Int. J. Thermal Sciences 57 (2012) 163-171.

[8] C. Lei, G. Xia, L. Wang, M. Zhou, Z. Cui, Heat transfer enhancement in microchannel heat sinks with periodic expansion-constriction cross-sections, Int. J. Heat Mass Transfer 62 (2013) 741-751.

[9] Islami, B. Dastvareh, R. Gharraei, Numerical study of hydrodynamic and heat transfer of nanofluid flow in microchannels containing micromixer, Int. Commun. Heat and Mass Transfer 43(2013)146-154.

[10] A. Heshmati, H. A. Mohammed, A. N. Darus, Mixed convection heat transfer of nanofluids over backward facing step having a slotted baffle, Applied Mathematics and Computation 240(2014) 368-386.

[11] H. E. Ahmed, M. Z. Yusoff, Delta- Winglet Pair of the vortex generators on the thermal and hydraulic performance of a triangular channel using Al2O3 –Water nanofluid, Int. J. of Heat transfer 136 (2014) 021901.
[12] M. Khoshvaght-Aliabadi, F. Hormozi, A. Zamzamian, Effects of geometrical parameters on performance of plate-fin heat exchanger: Vortex-generator as core surface and nanofluid as working media, Applied Thermal Engineering 70 (2014) 565-579.
[13] M. A. Ahmed, N. H. Shuaib, Yusoff, A. H. Al-Falahi, Numerical investigations of flow and heat transfer enhancement in a corrugated channel using nanofluid, Int. comm. Heat and Mass Transfer 38 (2011) 1368-1375.
[14] M. A. Ahmed, N. H. Shuaib and M. Z.Yusoff, Numerical investigations on the heat transfer enhancement in wavy channel using nanofluid, Int. J. Heat and Mass transfer 55 (2012) 5891-5898.
[15] M. A. Ahmed, M. Z.Yusoff and N. H. Shuaib, Effect of geometrical parameters on the flow and heat transfer characteristic in trapezoidal-corrugated channel using nanofluid, Int. comm. Heat and Mass Transfer 42 (2013) 69-74.
[16] M. A. Ahmed, M. Z.Yusoff, N. H. Shuaib, Effect of corrugation profile on the thermal-hydraulic performance of corrugated channel using CuO-water nanofluid, Case studied in thermal engineering 4 (2014) 65-75.
[17] M. A. Ahmed, M. Z.Yusoff, N. H. Shuaib, The effects of wavy-wall phase shift on thermal-hydraulic performance of Al_2O_3–water nanofluid flow in sinusoidal-wavy channel. Case studied in thermal engineering 4 (2014) 153-165.
[18] M. A. Ahmed, M. Z.Yusoff, N. H. Shuaib, Numerical and experimental investigation on the heat transfer enhancement in corrugated channels using SiO2-water nanofluid, Case studied in thermal engineering, Vol. 6, pp. 77-92, 2015.
[19] M. A. Ahmed, M. Z.Yusoff, K. C. Ng, N. H. Shuaib, Numerical investigations on the turbulent forced convection of nanfluids flow in a triangular-corrugated channel, Case studied in thermal engineering 6(2015) 212-225.
[20] H.A. Mohammed, O. A. Alawi, M.A.Wahid, Mixed convective nanofluid flow in a channel having backward-facing step with a baffle, Powder Technology 275 (2015) 329–343.
[21] A. Abdollahi, M. Shams, Optimization of heat transfer enhancement of nanofluid in a channel with winglet vortex generator, Applied Thermal Engineering 91(2015) 116-1126.
[22] J. Wang, Y. Zhao, Heat and fluid flow characteristics of a rectangular channel with a small diameter circular cylinder as vortex generator, Int. J. Thermal Sciences 92(2015) 1-13.
[23] M. H. Esfe, A. A. A. Arani, A. H. N., W. M. Yan, A. Karimipour, Mixed convection heat transfer from surface-mounted block heat sources in a horizontal channel with nanofluids, Int. J. Heat and Mass Transfer 89 (2015)783-791.
[24] M. Khoshvaght-Aliabadi, M. Khoshvaght, P. Rahnama, Thermal-hydraulic characteristics of plate-fin heat exchangers with corrugated/vortex-generator plate-fin (CVGPF), Applied Thermal Engineering 98 (2016) 690-701.
[25] A. Datta, D. Sanyal, A. K. Das, numerical investigation of heat transfer in microchannel using inclined longitudinal vortex generator, Applied Thermal engineering 108 (2016)1008-1019.
[26] T. K. Bose, Numerical fluid dynamic, Narosa Publishing House, London, 1997.
[27] A.S. Navaei, H.A. Mohammed, K.M. Munisamy, H. Yarmand, S. Gharehkhani, Heat transfer enhancement of turbulent nanofluid flow over various types of internally corrugated channels, Powder Technology 286 (2015) 332–341.
[28] H. K. Versteeg, W. Malalasekera, An introduction to computational fluid dynamics the finite volume method, 2nd edition Longman Scientific and Technical, England, 2007.
[29] J. H. Ferziger, M. Peric, Computational methods for fluid dynamics, 2nd edition. Springer-Verlag Berlin Heidelberg, New York, 1999.
[30] M. A. Ahmed, M. M. Yaseen, M. Z.Yusoff, Numerical study of convective heat transfer from tube bank in cross flow using nanofluid, Case studied in thermal engineering, 10 (2017) 560-569.
[31] S. E. Ghasemi, A.A. Ranjbar M.J. Hosseini, Numerical study on effect of CuO-water nanofluid on cooling performance of two different cross-sectional heat sinks, Advanced Powder Technology 28 (2017) 1495–1504.
[32] Y. Sui, P.S. Lee and C. J. Teo, An experimental study of the flow friction and heat transfer in wavy microchannels with rectangular cross section, Int. J. Thermal Sciences 50 (2011) 2473-2482.